

Fabrication and Characterization of $\text{Cu}_2\text{O}:\text{Ag}/\text{Si}$ Solar Cell Via Thermal Evaporation Technique

Alaa Nihad Tuama^{1*}, Khalid Haneen Abass², Mohd Arif Agam¹

¹Department of Physics, Faculty of Applied Sciences and Technology, University Tun Hussein Onn Malaysia, 84600 Pagoh, Johor, Malaysia.

²Department of Physics, College of Education for Pure Sciences, University of Babylon, Hillah, Iraq.

Received 28 April 2020, Revised 21 July 2020, Accepted 18 August 2020

ABSTRACT

Cuprous oxide, a p-type semiconductor, permits multiple device applications due to the non-toxic nature, suitable direct energy gap, earth abundance, and ideal band alignment needed for solar cell and photoelectrochemical applications. Due to that, there has been a renewal of interest in solar cells fabrication field based on Cu_2O material. In this work, pure cuprous oxide and silver nanoparticles doped cuprous oxide (0.02, 0.04, 0.06 wt.%) films were prepared via thermal evaporation technique with a thickness of 60 nm. The structural, morphological, optical, and electrical properties of the films have been studied by characterization instruments such as X-ray Diffraction (XRD), Field Emission Scanning Electron Microscope (FESEM), Atomic Force Microscope (AFM), UV-Visible spectrophotometer, and I-V characteristic. The XRD revealed that the fabricated films have a certain amorphous quality and the grain size was found to be in between (9.2-18.4) nm which comparable to that measured from FESEM. The optical bandgap of the samples was found to be in between 2.79 eV and 3.42 eV which was the main factor in manipulating and improving the Cu_2O optical properties by doping and choosing the appropriate ones to fabricate high efficiency and low-cost solar cells. The effect of the Ag doping on the Cu_2O properties was obvious and positively influenced by solar cell efficiency improvement. Optimization of the deposition conditions and doping process led to enhanced solar cell performance, especially the conversion efficiency achieved (3.5) by doping 0.04% Ag to Cu_2O which is considered to be highly efficient compared to the overall efficiency of Cu_2O solar cells. This can open a new route for the fabrication of Cu_2O based solar cells with improved performance.



Graphical Abstract

Keywords: Cuprous Oxide, Solar Cell, FESEM, Thermal Evaporation Technique.

*Corresponding Author: aalaa_nihad@yahoo.com

1. INTRODUCTION

Solar energy is considered the cleanest, unlimited, and low-cost energy source despite the dominance of fossil fuels through the last decades. One of the solar energy types is semiconducting-based solar cells that currently dominates the solar energy field due to relatively high developed fabrication methods and well power conversion efficiencies [1]. Copper oxide is one of the semiconductors that is widely used in solar cell fabrication which has two stable types: cupric oxide (CuO) and cuprous oxide (Cu₂O) [2]. Cuprous oxide is a p-type semiconductor material with 2.17 eV direct band gap [3]. The basic interesting characteristic of (Cu₂O) is low-cost, non-toxic, high stability [4], environmentally benign, large optical absorption, high carrier mobility, and abundance of the resources [5-10]. Due to these interesting properties, Cu₂O has been widely used as an active layer in solar cell fabrication. A p-type cuprous oxide heterojunction (HJ) solar cells (p-Cu₂O) has been intensively investigated [11-16] due to the difficulty of preparing a suitable n-type Cu₂O. Furthermore, Cu₂O HJ solar cells could realize a photoelectric conversion efficiency theoretically of 20% (under AM1 illumination) by using several kinds of formation methods and solar cell fabrication techniques [17]. Cuprous oxide thin films have been widely prepared by various techniques such as electrodeposition [18-19], PLD [20-21], radio-frequency magnetron sputtering [22], thermal oxidation [23-24], and thermal evaporation [25-26], [2]. Thermal evaporation of cuprous oxide powder (99.9%) high purity is one method which can produce high quality and well-distributed Cu₂O films doped with very small ratios of silver. In this work, thin films are prepared from pure cuprous oxide and silver doped cuprous oxide through thermal evaporation technique. The effect of the thickness and ratio of Ag on the optical, electrical, and structural properties has been studied. Fabrication of Cu₂O:Ag/Si heterojunction solar cell and its efficiency also has been studied.

2. EXPERIMENTAL

Preparation and characterization of pure Cu₂O and Ag-doped Cu₂O thin films with various doping concentrations (0.02, 0.04, and 0.06) wt.% via thermal evaporation method on silicon and glass substrates were done. Modified Edward C-306 is the system used for the thermal evaporation process. The Cu₂O powder of 99.9% purity (40 nm particle size) and Ag powder of 99.9% purity (20-30 nm particle size) were used as starting materials on a boat of molybdenum. The chamber was subjected to evacuation down to 1×10^{-7} mbar by using this modified version of Edward C-306 system. The distance between the source and substrate was about 15 cm. The prepared films were annealed at a temperature of 573 K for 2 hours. The structural properties of the films were characterized by (XRD-6000) SHIMADZU X-ray Diffractometer (XRD) system with a source CuK α and radiation of wavelength $\lambda = 1.5406 \text{ \AA}$ and the Field Emission Scanning Electron Microscope (FESEM) was used to determine the shape and size of the prepared (Cu₂O:Ag) thin films. The roughness of the surface was characterized by a scanning probe microscope (A α 3000 AFM) and the recording of the absorbance spectra of the films have been done by using a spectrophotometer (Shimadzu UV-1650 PC) made by Phillips (Japan) in the wavelength range 200 to 1100 nm, based on Van der Pau method. The electrical properties were characterized by (I-V characteristics) and the thickness was measured by optical thin film measurements with lambda Limf-10 and calculated by weight method using Equation 1:

$$t = \frac{m}{2\pi\rho R^2} \quad (1)$$

where t is the thickness of the thin films (nm), m is the mass of the material in (g), ρ is the density of material (g/cm^3), and R is the distance between the substrate and the boat (cm). The two results were comparable to be 60 nm. Masking techniques, usually formed by a metal (Al foils) were used to fabricate the front and back contacts of the solar cell. These masks are placed as

closely as possible to the films to deposit the electrodes of the solar cell by using the same evaporation technique.

3. RESULTS AND DISCUSSION

3.1 Structural Characterization

Since the structural nature of semiconductor materials is a vital factor in fabricating solar cells and other applications. X-ray Diffraction (XRD) patterns of the Cu_2O thin films have been recorded. The X-ray diffraction for un-doped and Ag-doped Cu_2O is illustrated in Figure 1. From XRD pattern, three peaks were found at $2\theta = (31.22^\circ, 38.25^\circ, 44.23^\circ)$ which corresponds to the $\{(110), (111), (200)\}$ respectively. This indicates that the cuprous oxide, undoped and silver doped films fabricated via vacuum evaporation technique, exhibited a good cubic direction normal to the substrate, from basic planes of cubic Cu_2O with equivalent intensity were observed, which meant the dense films were composed of Cu_2O grains. Polycrystalline films can be recognized from the peaks that appear in pure Cu_2O , while the peaks were started to disappear with Ag-doping to convert the films to amorphous. Table 1 shows the obtained results of X-ray diffraction for the silver doped cuprous oxide films. The crystallite-size D of the Ag-doped Cu_2O films was calculated by using Scherrer's formula in Equation 2 [27]:

$$D = 0.9\lambda / (\beta \cos\theta) \quad (2)$$

Where β is the full width at half maximum (radian), λ is the X-ray wavelength (\AA), and θ is the Bragg diffraction angle of the XRD peak (degree). The crystallite size that calculated from Scherrer's formula ranged from 9.2 - 18.4 nm tabulated in Table 1.

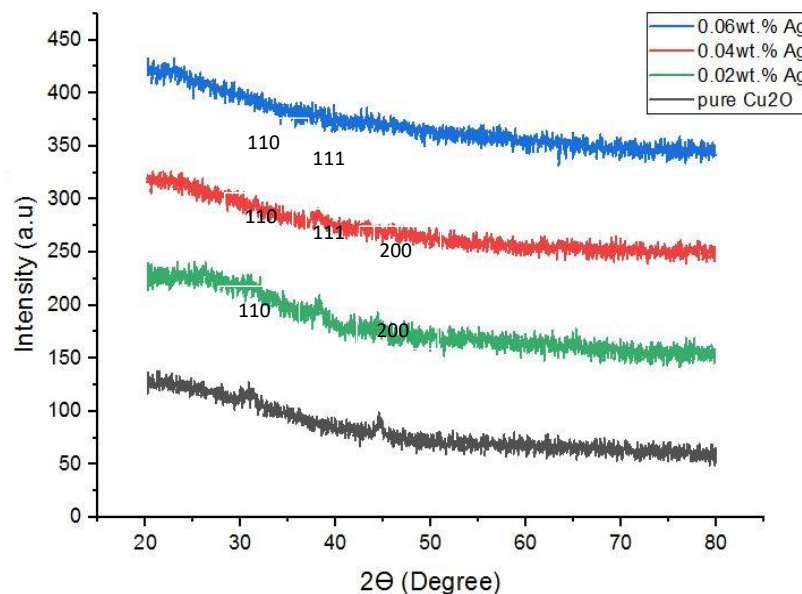
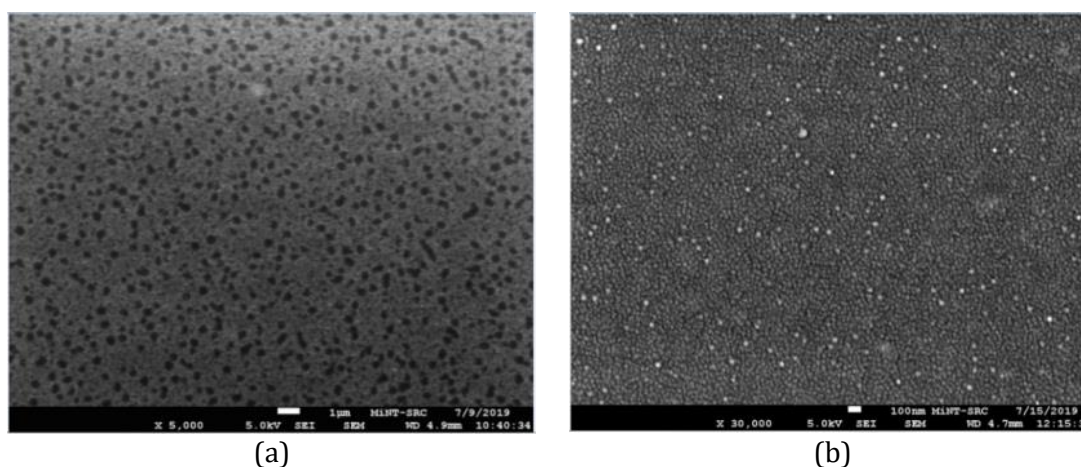


Figure1. XRD patterns of Ag-doped Cu_2O films.

Table 1 The obtained results of XRD for Ag-doped Cu₂O thin film

Ag-doped Cu ₂ O (wt.%)	2θ (degree)	hkl	FWHM (degree)	Crystallite size (nm)
0.00	30.82	110	0.275	18.4
	44.75	200	0.461	10.6
0.02	30.84	110	0.278	18.0
	38.45	111	0.390	15.0
	44.75	200	0.375	9.2
0.04	31.50	110	0.288	16.1
	38.45	111	0.282	13.2
0.06	-	-	-	-

The shape and size of the nanoparticles of prepared films were determined by FESEM. The deposition of the pure and Ag-doped Cu₂O on a glass substrate is shown in Figure 2. It can be observed that the morphologies of the films surface significantly changed after deposition depending on the Ag doping in the prepared films and the crystallinity of the films is possibly affected by the Ag doping and substrates used for deposition. Images of the undoped and Ag-doped Cu₂O films as in series of images in Figure 2 indicated of smooth surfaces with no pinholes that the nanoparticles are found in the range of 18-24 nm. Also, the increasing in Ag nanoparticles at specific places indicates a regular distribution of nanoparticles during the time of the deposition process. Similar results are comparable with this report as the homogenous Ag nanoparticles distribution is vital in increasing the solar cell efficiency due to the surface plasmonic property in nanostructures or thin films of noble metals [28]. This FESEM images showed that the magnified view of the fabricated films had a spherical morphology which revealed the well-distributed nanoparticles. Most of the particles have approximately the same size. However, few larger spherical and semi-spherical particles were also present possibly due to the effect of vacuum deposition and distribution with the absence of defect and holes in these films.



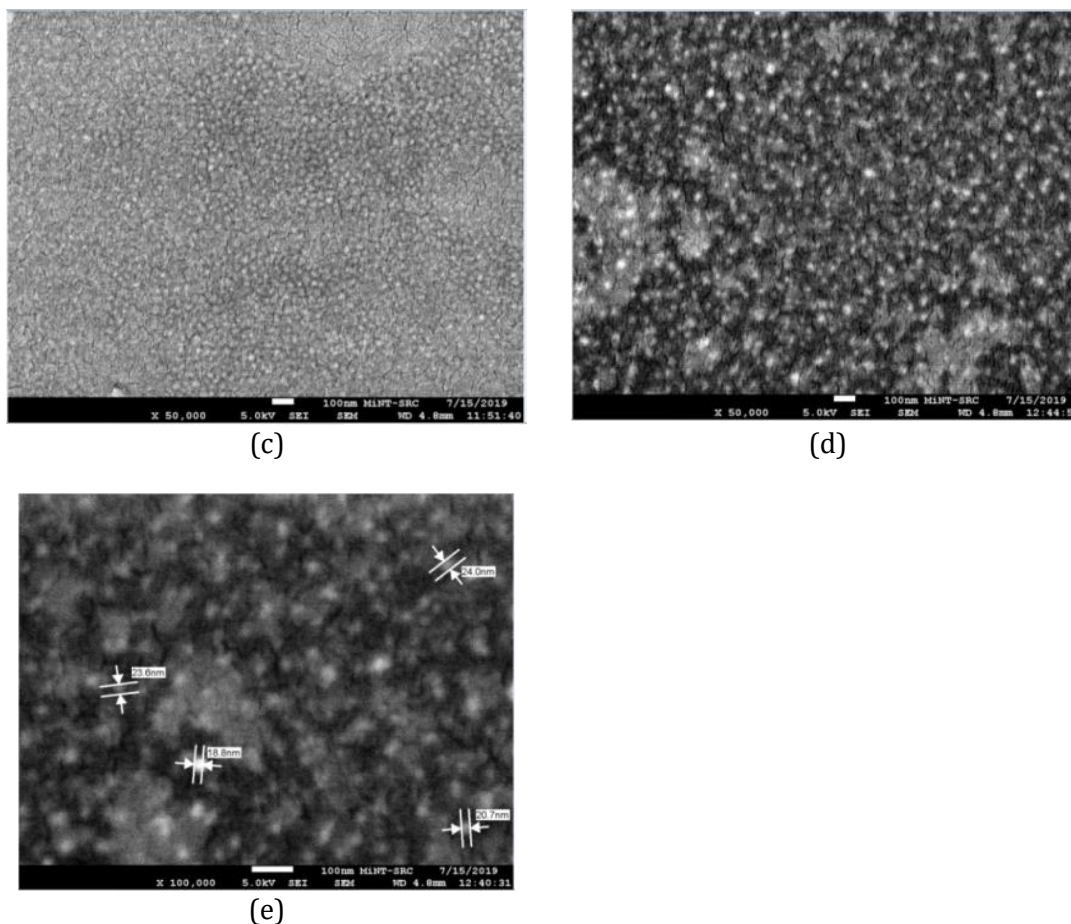


Figure 2. FESEM images of the undoped and Ag-doped Cu_2O films prepared by thermal evaporation technique where (a) pure cuprous oxide, (b) 0.02%Ag doped cuprous oxide, (c) 0.04%Ag doped cuprous oxide, and (d-e) 0.06%Ag doped cuprous oxide films).

The films of Cu_2O and Ag-doped Cu_2O were complimented with AFM images. Figure 3 shows the surface images of Cu_2O films on glass substrate combined with the histogram graphs. The AFM scanning images of the films revealed a uniform surface morphology with granular form, as the surface roughness is found to be increased from 0.332 nm for pure Cu_2O to 1.720 for $\text{Cu}_2\text{O}:0.06\%$ Ag films. The increase in roughness can be attributed to the increased concentration of silver nanoparticles in the Cu_2O nanofilms [28-29]. For the prepared Cu_2O films, the surface is smooth and composed of small grains and the root mean square (RMS) values increased from 0.427 nm for pure Cu_2O to 2.12 nm for $\text{Cu}_2\text{O}:0.06\%$ Ag nanofilms. The results are listed in Table 2.



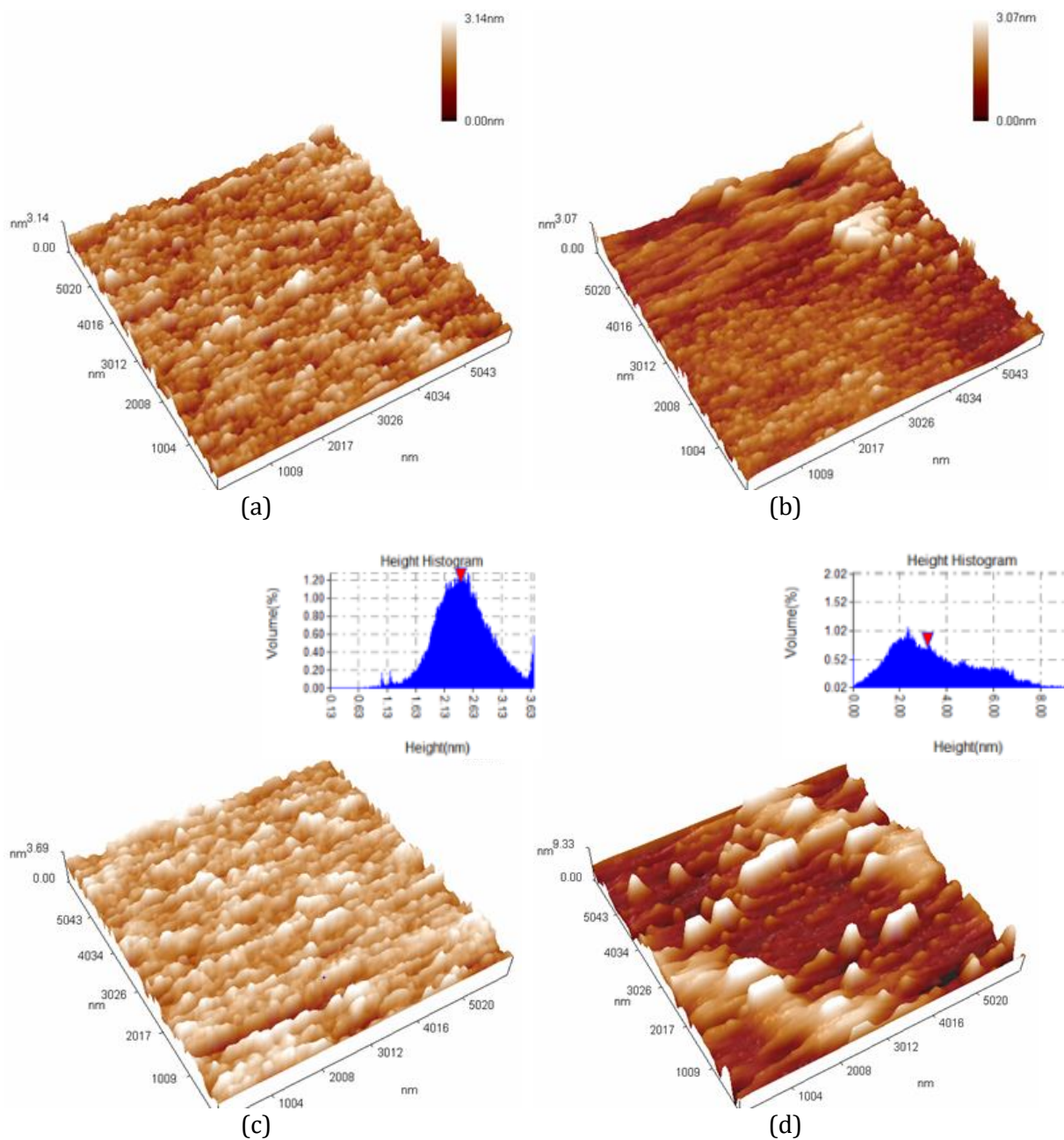


Figure 3. The AFM images of (a) pure cuprous oxide, (b) 0.02% Ag doped cuprous oxide, (c) 0.04% Ag doped cuprous oxide, and (d) 0.06% Ag doped cuprous oxide films.

Table 2 Morphological characteristics of Cuprous oxide: silver nanofilms at annealing temperature 573 K and various Ag-doping

Film	Roughness average (nm)	Root mean square (nm)	Ten-point height (nm)
Cu ₂ O	0.332	0.427	1.52
Cu ₂ O:0.02%Ag	0.311	0.420	2.98
Cu ₂ O:0.04%Ag	0.389	0.497	3.54
Cu ₂ O:0.06%Ag	1.72	2.120	9.32

3.2 Optical Characterization

The optical properties of the pure and Ag-doped Cu₂O with various Ag doping (0.02, 0.04, 0.06) wt.% films were calculated from recording the absorbance in the wavelength range (190-1100) nm using UV-Visible spectrophotometer. The absorbance spectra versus wavelength of the films were presented in Figure 4. The figure shows the absorption spectra of the pure and Ag-doped Cu₂O films, which increases with the increasing of Ag doping resulting from the formation of secondary levels inside the energy gap.

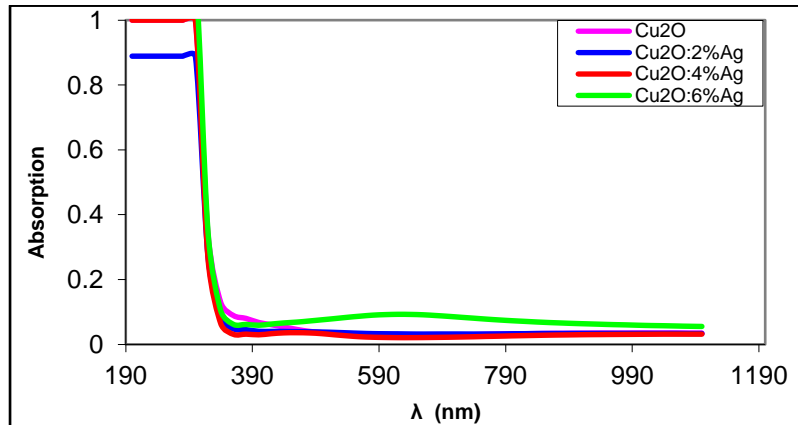


Figure 4. Absorbance spectra of the pure and Ag-doped Cu₂O films.

The absorption coefficient (α) was determined from the region of high absorption at the fundamental absorption edge of the film using the relation in Equation 3 [30]:

$$\alpha = 2.303 \frac{A}{t} \quad (3)$$

Where A is the absorbance and t are the thickness of the film. The absorption coefficient versus wavelength was presented in Figure 5. It can be observed that the absorbance increases with the increasing of Ag doping for the prepared films. The values were greater than $10^4/\text{cm}$, which led to the increase of probability of the appearance of direct transfers. This can be related to the decrease the grain size and it can be attributed to the scattering of light for its increasing surface-roughness [29],[31].

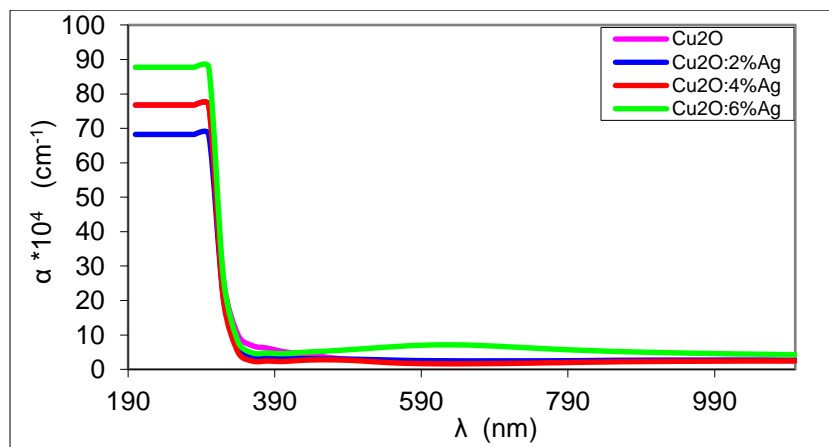


Figure 5. The absorption coefficient of the pure and Ag-doped Cu₂O films.

The optical energy gap was determined by Equation 4 [32]:

$$(\alpha h\nu) \approx [h\nu - E_g]n \quad (4)$$

The plot of $(\alpha h\nu)^2$ versus photon energy ($h\nu$) indicates that the Cu₂O films are semiconductors of direct transition type. Figure 6 shows the energy gap of pure and Ag-doped Cu₂O films with various doping concentrations of Ag (0.02, 0.04, and 0.06) wt.%. As shown in Figure 6, the energy gap was determined by extrapolating the linear portion of the plot. It can be observed that the energy gap has changed significantly with increasing Ag doping, this attributed to the very thin films prepared on a glass substrate [31]. The energy gap values for the prepared films were ranged from 2.79-3.42 eV (2.79 eV for Cu₂O film and 3.21 eV for 0.06 wt.% Ag-doped Cu₂O film), this behaviour in agreement with the finding by researchers [33]. The increasing and decreasing in energy gap can be justified by the pre-position that the Cu₂O:Ag films are semiconductors in which the Fermi level located in the conduction band, which means that the electrons occupied the bottom of the conduction band. The shielding electrons moving to these levels causing to the electrons travelling from the valence to conduction bands which are defined as the Burstein Moss effect [32].

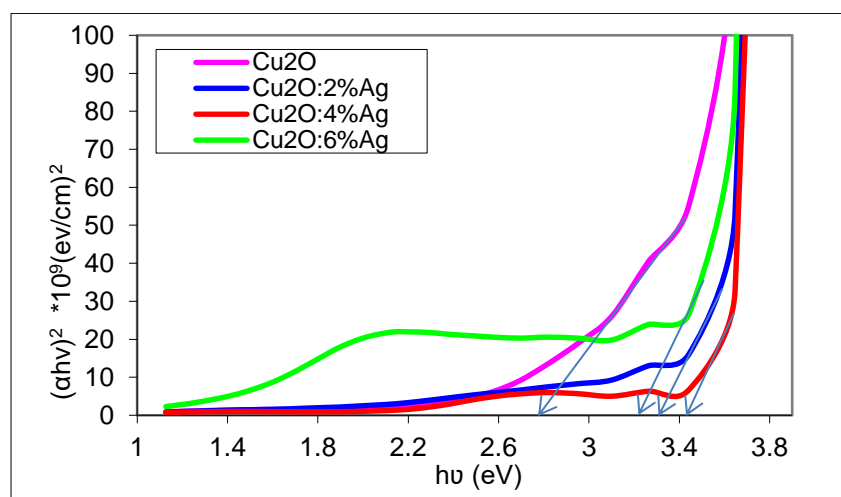


Figure 6. The optical bandgap of the pure Cu₂O and Ag-doped Cu₂O films.

3.3 Electrical Characterization

The C–V measurements were performed to obtain information about the semiconductor doping concentration, the potential barrier at the junction and the presence of traps in materials. The plots of $1/C^2$ with a reverse bias of Cu₂O:Ag/Si solar cells with various doping ratios are shown in Figure 7. The width of the potential barrier in each region can be deduced from Figure 7, which is confirming that the junction quality is not lost using the thermal evaporation fabrication. The built-in potential (V_{bi}) and donor concentration (N_D) were evaluated from the slope and the intercept of $1/C^2$ versus V , respectively. The built-in potential (V_{bi}) can be determined from extrapolating of $(1/C^2 - V)$ plot to $((1/C^2) = 0)$ [34-35]. Table 3 shows the values of V_{bi} calculated of Cu₂O:Ag/Si solar cells prepared at various Ag doping.

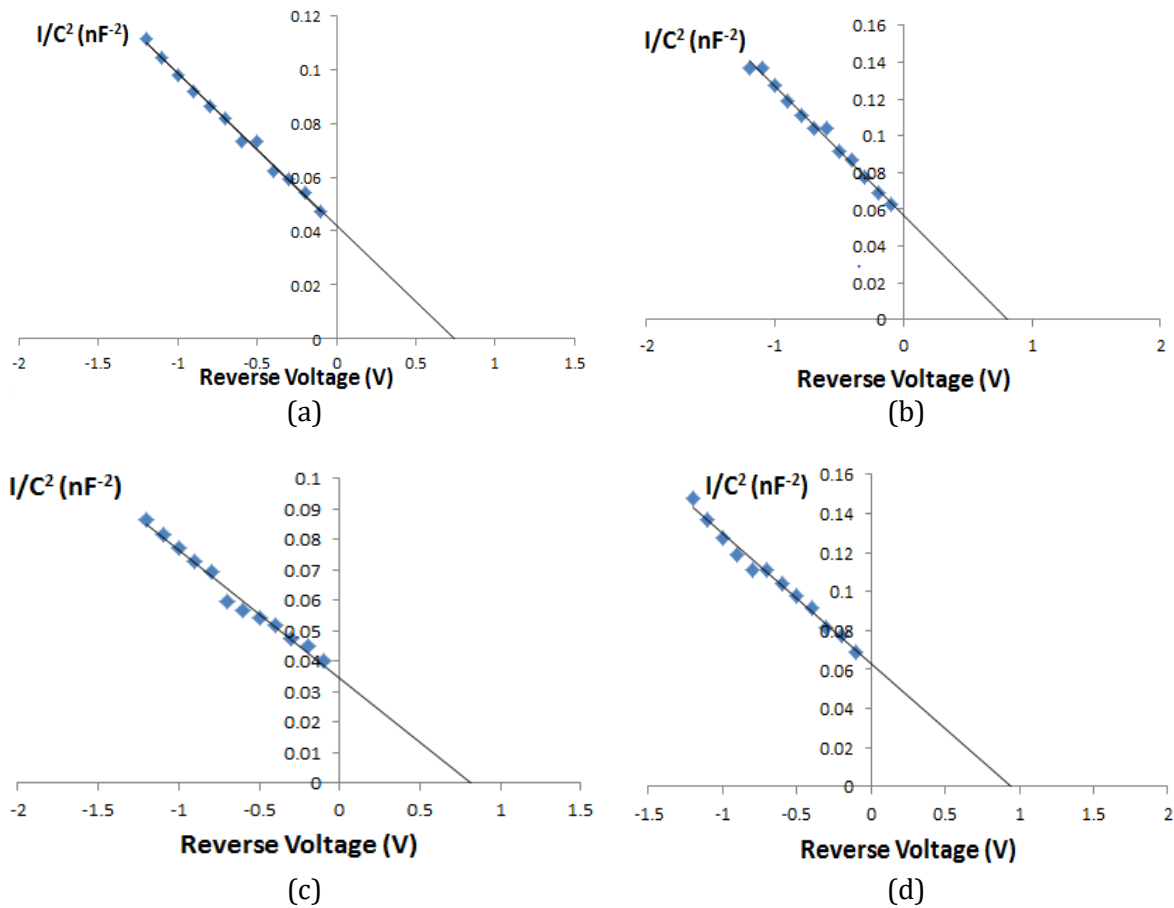


Figure 7. The plot of $1/C^2$ versus reverse voltage for $\text{Cu}_2\text{O}:\text{Ag}/\text{Si}$ with various Ag doping.

Table 3 Built-in potential for $\text{Cu}_2\text{O}:\text{Ag}/\text{Si}$ heterojunction

Fabricated Solar Cells	V_{bi}
$\text{Cu}_2\text{O}/\text{Si}$	0.75
$\text{Cu}_2\text{O}:\text{0.02Ag}/\text{Si}$	0.8
$\text{Cu}_2\text{O}:\text{0.04 Ag}/\text{Si}$	0.81
$\text{Cu}_2\text{O}:\text{0.06 Ag}/\text{Si}$	0.86

The I-V curves of the p- $\text{Cu}_2\text{O}:\text{Ag}/\text{n-Si}$ heterojunctions are illustrated in Figure 8. The solar cell efficiency can be evaluated from the I-V curves. For the fabrication and characterization of p-n junction devices, front and back contacts of the solar cell are fabricated by depositing pure aluminium on the $\text{Cu}_2\text{O}:\text{Ag}/\text{Si}$ films. The I-V of $\text{Cu}_2\text{O}:\text{Ag}/\text{n-Si}$ heterojunction were characterized at a voltage of forward bias for various Ag doping within the range of (-1.5 V to 1.5 V). These curves demonstrated the behaviour of the current with the reverse and forward bias voltage. The characteristics of voltage and current under illumination were one of the vital optoelectronic parameters for heterojunctions, the calculations were performed under densities of incident power equal to $100 \text{ mW}/\text{cm}^2$. The increasing in the photocurrent with the increasing of bias voltage can be obtained from the I-V curves. It can also be observed that the photocurrent in the backward bias was higher than that in the forward bias. This could be attributed to the fact that the width of the depletion region increased with the increasing of the reverse bias applied voltage that caused to the separation of the electrons and holes pairs.

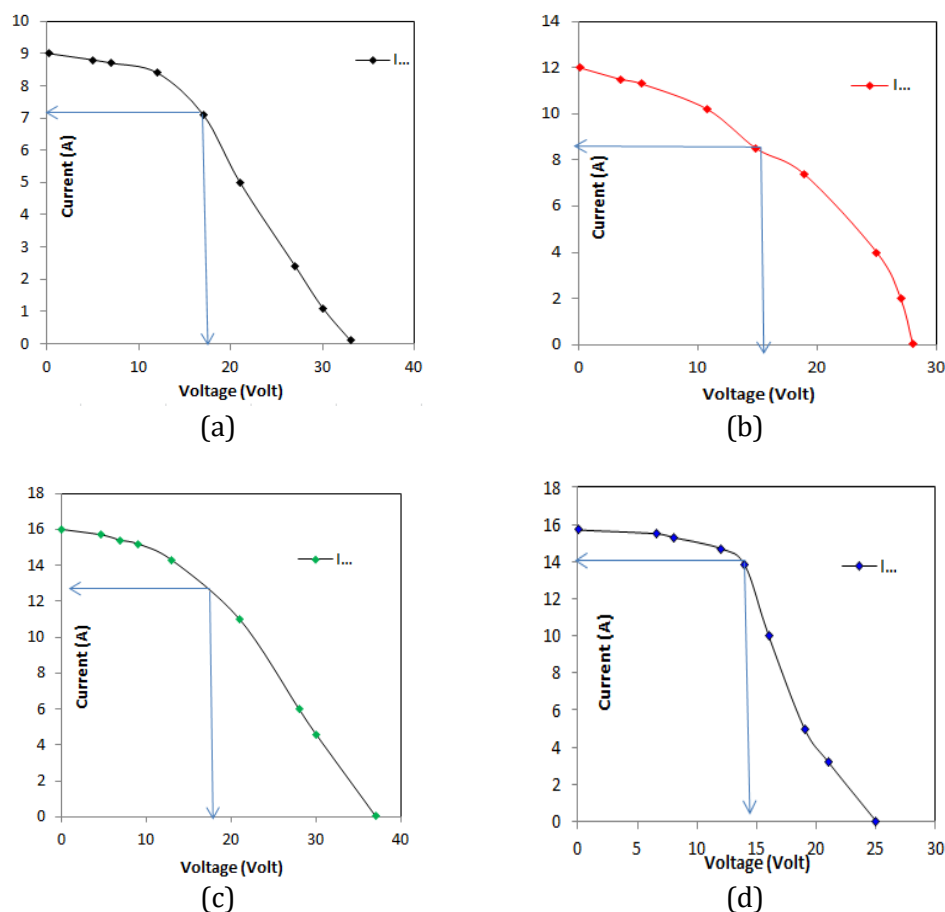


Figure 8. The I-V characteristics of Ag-doped Cu₂O/Si solar cells with P=100 mW/cm² of: (a) Cu₂O/Si, (b) 0.02% Ag-doped Cu₂O/Si, (c) 0.04% Ag-doped Cu₂O/Si, and (d) 0.06% Ag-doped Cu₂O/Si.

The efficiency of the solar cell increased with increasing of Ag doping. The highest efficiency is 3.5 at 0.04 wt.% Ag doping with short circuit current (I_{sc}) of 0.16 mA, open-circuit voltage (V_{oc}) of 37.5 V, and full factor 0.38. All calculated values are listed in Table 4. The enhanced solar cell performance can be attributed to the low ratios of Ag doping, which is considered as the fundamental factor used to manipulate the cuprous oxide nanofilms properties, especially the optical and electrical properties. The solar cell efficiency achieved in this work yield a good value despite the absence of the dye as well as the absence of various layers in the prepared solar cell.

Table 4. Results of I-V for Ag-doped Cu₂O thin films with various doping at room temperature.

Pure and Ag doped Cu ₂ O (wt.%)	I _{sc} (mA/cm ²)	V _{oc} (volt)	I _{max} (mA)	V _{max} (volt)	F.F	η (%)
Cu ₂ O	0.09	33.0	0.071	17.5	0.42	2.1
0.02	0.12	28.0	0.085	16.0	0.40	2.3
0.04	0.16	37.5	0.125	18.0	0.38	3.8
0.06	0.16	25.0	0.140	14.5	0.34	3.5

4. CONCLUSION

In summary, four samples of cuprous oxide and silver doped cuprous oxide films were thermally evaporated on glass and silicon substrates with a thickness of 60 nm. From XRD, the polycrystalline and amorphous was satisfied with a cubic orientation structure perpendicular to

the substrate. The crystallite size decreased slightly with the increasing of Ag doping. The morphology characterization of the pure and Ag-doped cuprous oxide films at various Ag concentrations showed a uniform granular surface morphology and the roughness average combined with root mean square increased with the increasing of Ag doping. The optical properties of the prepared films showed that the pure and Ag-doped Cu₂O films allowed a direct energy gap (E_g) that increased from 2.79 to 3.42 eV. The FESEM images showed that the magnified view and the spherical morphology is manifest which is revealed the well-distributed nanoparticles. Most of the particles were of the same size and few of them were larger. The highest conversion efficiency (η) was 3.8% for 0.04% Ag-doped Cu₂O thin film. Control of nanoscale thickness and particle size to obtain properties different from the traditional work of copper oxide led to a marked improvement in the efficiency of the prepared solar cell. This work shows that the proposed strategy to enhance the performance of the solar cell realized by thermal evaporation deposition.

ACKNOWLEDGMENT

This work was funded by the Fundamental Research Grant awarded by the Ministry of Education (FRGS K171) and TIER 1 (H218) and GPPS (H423), awarded by University Tun Hussein Onn (UTHM), Malaysia.

REFERENCES

- [1] Cui, Jingbiao, and Ursula J. Gibson. A Simple Two-Step Electrodeposition of Cu₂O/ZnO Nanopillar Solar Cells. *Journal of Physical Chemistry C* **114**, 14 (2010) 6408–12. <https://doi.org/10.1021/jp1004314>.
- [2] Al-Kuhaili, M. F. Characterization of Copper Oxide Thin Films Deposited by the Thermal Evaporation of Cuprous Oxide (Cu₂O). *Vacuum* **82**, 6 (2008) 623–29. <https://doi.org/10.1016/j.vacuum.2007.10.004>.
- [3] Chen, Lung Chien. Review of Preparation and Optoelectronic Characteristics BN of Cu₂O-Based Solar Cells with Nanostructure. *Materials Science in Semiconductor Processing* **16**, 5 (2013) 1172–85. <https://doi.org/10.1016/j.mssp.2012.12.028>.
- [4] Liu, Yingchi, Hubert K. Turley, John R. Tumbleston, & Rene Lopez. 2011. Minority Carrier Transport Length in Electrodeposited Cu₂O for Heterojunction Solar Cells. *Thin Film Solar Technology III* 8110: 81100P. <https://doi.org/10.1117/12.892123>.
- [5] McShane, Colleen M., Withana P. Siripala, and Kyoung Shin Choi. “Effect of Junction Morphology on the Performance of Polycrystalline Cu₂O Homojunction Solar Cells.” *Journal of Physical Chemistry Letters* **1**, 18 (2010) 2666–70. <https://doi.org/10.1021/jz100991e>.
- [6] Thi Ha, T., Thi Huyen Trang, N., Thanh Cong, B., Dieu Thu, N. T., Thanh Binh, N., Viet Tuyen, N., & Nguyen Hai, P. Effect of Annealing Temperature on Cu₂O Thin Films Prepared by Thermal Oxidation Method. *VNU Journal of Science: Mathematics - Physics* **36**, 2 (2020) 31–36. <https://doi.org/10.25073/2588-1124/vnumap.4426>
- [7] Abdelfatah, M., Ismail, W., El-Shafai, N. M., & El-Shaer, A. Effect of thickness, bandgap, and carrier concentration on the basic parameters of Cu₂O nanostructures photovoltaics: numerical simulation study. *Materials Technology* **00**, 00 (2020) 1–9. <https://doi.org/10.1080/10667857.2020.1793092>
- [8] Tuama, A. N., Abass, K. H., Hamzah, M. Q., Mezan, S. O., & Bin Agam, M. A. Morphological and optical properties of cuprous oxide nano films for solar cell application. *Test Engineering and Management* **83**, 13090 (2020) 13090–13099.
- [9] Miyata, T., Tokunaga, H., Watanabe, K., Ikenaga, N., & Minami, T. Photovoltaic properties of low-damage magnetron-sputtered n-type ZnO thin film/p-type Cu₂O sheet heterojunction solar cells. *Thin Solid Films*, 697 (August 2019) (2020) 137825. <https://doi.org/10.1016/j.tsf.2020.137825>

- [10] Naveen Kumar, J., Thanikaikarasan, S., & Roji Marjorie, S. Electrochemical growth and characterization of Cu₂O thin films. *Materials Today: Proceedings*, (xxxx), (2020). <https://doi.org/10.1016/j.matpr.2020.05.226>
- [11] Noda, S., H. Shima, & H. Akinaga. 2013. Cu₂O/ZnO Heterojunction Solar Cells Fabricated by Magnetron-Sputter Deposition Method Films Using Sintered Ceramics Targets. *Journal of Physics: Conference Series* 433 (1). <https://doi.org/10.1088/1742-6596/433/1/012027>.
- [12] Hoye, Robert L.Z., Riley E. Brandt, Yulia Ievskaya, Shane Heffernan, Kevin P. Musselman, Tonio Buonassisi, and Judith L. Macmanus-Driscoll. Perspective: Maintaining Surface-Phase Purity Is Key to Efficient Open Air Fabricated Cuprous Oxide Solar Cells. *APL Materials* 3, 2 (2015) <https://doi.org/10.1063/1.4913442>.
- [13] Ievskaya, Y., R. L.Z. Hoye, A. Sadhanala, K. P. Musselman, & J. L. MacManus-Driscoll. Fabrication of ZnO/Cu₂O Heterojunctions in Atmospheric Conditions: Improved Interface Quality and Solar Cell Performance. *Solar Energy Materials and Solar Cells* 135 (2015) 43–48. <https://doi.org/10.1016/j.solmat.2014.09.018>.
- [14] Minami, Tadatsugu, Yuki Nishi, & Toshihiro Miyata. “Heterojunction Solar Cell with 6% Efficiency Based on an N-Type Aluminum-Gallium-Oxide Thin Film and p-Type Sodium-Doped Cu₂O Sheet.” *Applied Physics Express* 8, 2 (2015) 022301. <https://doi.org/10.7567/APEX.8.022301>.
- [15] Lee, Sang Woon, Yun Seog Lee, Jaeyeong Heo, Sin Cheng Siah, Danny Chua, Riley E. Brandt, Sang Bok Kim, Jonathan P. Mailoa, Tonio Buonassisi, & Roy G. Gordon. Improved Cu₂O-Based Solar Cells Using Atomic Layer Deposition to Control the Cu Oxidation State at the p-n Junction. *Advanced Energy Materials* 4, 11 (2014) 1–7. <https://doi.org/10.1002/aenm.201301916>.
- [16] Lee, Yun Seog, Danny Chua, Riley E. Brandt, Sin Cheng Siah, Jian V. Li, Jonathan P. Mailoa, Sang Woon Lee, Roy G. Gordon, & Tonio Buonassisi. Atomic Layer Deposited Gallium Oxide Buffer Layer Enables 1.2 v Open-Circuit Voltage in Cuprous Oxide Solar Cells. *Advanced Materials* 26, 27 (2014) 4704–10. <https://doi.org/10.1002/adma.201401054>.
- [17] Minami, Tadatsugu, Toshihiro Miyata, & Yuki Nishi. “Efficiency Improvement of Cu₂O-Based Heterojunction Solar Cells Fabricated Using Thermally Oxidized Copper Sheets.” *Thin Solid Films* 559 (2014) 105–11. <https://doi.org/10.1016/j.tsf.2013.11.026>.
- [18] Nishi, Yuki, Toshihiro Miyata, & Tadatsugu Minami. “Electrochemically Deposited Cu₂O Thin Films on Thermally Oxidized Cu₂O Sheets for Solar Cell Applications.” *Solar Energy Materials and Solar Cells* 155 (2016) 405–10. <https://doi.org/10.1016/j.solmat.2016.06.013>.
- [19] Wijesundera, R. P., L. K. A. D. S. Gunawardhana, & W. Siripala. “Electrodeposited Cu₂O Homojunction Solar Cells: Fabrication of a Cell of High Short Circuit Photocurrent.” *Solar Energy Materials and Solar Cells* 157 (2016) 881–86. <https://doi.org/10.1016/j.solmat.2016.07.005>.
- [20] Hossain, Md Anower, Rashad Al-Gaashani, Hicham Hamoudi, Mohammed J. Al-Marri, Ibnelwaleed A. Hussein, Abdelhak Belaidi, Belabbes A. Merzougui, Fahhad H. Alharbi, & Nouar Tabet. “Controlled Growth of Cu₂O Thin Films by Electrodeposition Approach.” *Materials Science in Semiconductor Processing* 63 (November 2016) (2017) 203–11. <https://doi.org/10.1016/j.mssp.2017.02.012>.
- [21] Wee, Sung Hun, Po Shun Huang, Jung Kun Lee, & Amit Goyal. “Heteroepitaxial Cu₂O Thin Film Solar Cell on Metallic Substrates.” *Scientific Reports* 5 (2015) 3–9. <https://doi.org/10.1038/srep16272>.
- [22] Sawant, Sachin S., Ashok D. Bhagwat, & Chandrashekhar M. Mahajan. “Synthesis of Cuprous Oxide (Cu₂O) Nanoparticles - A Review.” *Journal of Nano- and Electronic Physics* 8, 1 (2016) 1–5. [https://doi.org/10.21272/jnep.8\(1\).01035](https://doi.org/10.21272/jnep.8(1).01035)
- [23] Chen, Sujuan, Limei Lin, Jinyang Liu, Peiwei Lv, Xiaoping Wu, Weifeng Zheng, Yan Qu, & Fachun Lai. “An Electrochemical Constructed P-Cu$\langle 2 \rangle / \langle n \rangle$-ZnO Heterojunction for Solar Cell.” *Journal of Alloys and Compounds* 644 (2015) 378–82. <https://doi.org/10.1016/j.jallcom.2015.02.230>.

- [24] Ohajianya, A. C., & O. E. Abumere. "Effect of Cuprous Oxide (Cu₂O) Film Thickness on the Efficiency of the Copper-Cuprous Oxide (Cu₂O/Cu) Solar Cell." *The International Journal Of Engineering And Science* **2**, 5 (2013) 42–47. www.theijes.com.
- [25] Chen, Cheng Chiang, Lung Chien Chen, & Yi Hsuan Lee. "Fabrication and Optoelectrical Properties of IZO/Cu₂O Heterostructure Solar Cells by Thermal Oxidation." *Advances in Condensed Matter Physics* 2012, (2012). <https://doi.org/10.1155/2012/129139>.
- [26] Gevorkyan, V. A., A. E. Reymers, M. N. Nersesyan, & M. A. Arzakantsyan. "Characterization of Cu₂O Thin Films Prepared by Evaporation of CuO Powder." In *Journal of Physics: Conference Series*. **350** (2012). <https://doi.org/10.1088/1742-6596/350/1/012027>.
- [27] Abass, Khalid Haneen, Mohammed Hadi Shinen, & Ayad F. Alkaim. "Preparation of TiO₂ Nanolayers via. Sol-Gel Method and Study the Optoelectronic Properties As solar Cell Applications." *Journal of Engineering and Applied Sciences* **13**, 22 (2018) 9631–37. <https://doi.org/10.3923/jeasci.2018.9631.9637>.
- [28] Haneen Abass, Khalid, & Noor Haidar Obaid. "0.006wt.%Ag-Doped Sb₂O₃ Nanofilms with Various Thickness: Morphological and Optical Properties." In *Journal of Physics: Conference Series*. **1294** (2019). <https://doi.org/10.1088/1742-6596/1294/2/022005>.
- [29] Hassan, Ehssan S., Tahseen H. Mubarak, Khalid H. Abass, Sami S. Chiad, Nadir F. Habubi, Maher H. Rahid, Abdulhussain A. Khadayeir, Mohamed O. Dawod, & Ismaeel A. Al-Baidhany. "Structural, Morphological and Optical Characterization of Tin Doped Zinc Oxide Thin Film by (SPT)." In *Journal of Physics: Conference Series*. **1234** (2019). <https://doi.org/10.1088/1742-6596/1234/1/012013>.
- [30] Chopra, K., & Julius Klerrer. "Thin Film Phenomena." *Journal of The Electrochemical Society* **117**, 5 (1970) 180C. <https://doi.org/10.1149/1.2407581>.
- [31] Hill, R. M. "Thin Film Phenomena." *Thin Solid Films* **5**, 3 (1970) 199. [https://doi.org/10.1016/0040-6090\(70\)90077-5](https://doi.org/10.1016/0040-6090(70)90077-5).
- [32] Abass, Khalid Haneen, & Musaab Khudhur Mohammed. "Nano Biomed Eng Fabrication of ZnO : Al / Si Solar Cell and Enhancement Its Efficiency Via Al-Doping" **11**, 2 (2019) 170–77. <https://doi.org/10.5101/nbe.v11i2.p170-177.Research>.
- [33] Akgul, Funda Aksoy, Guvenc Akgul, Nurcan Yildirim, Husnu Emrah Unalan, & Rasit Turan. "Influence of Thermal Annealing on Microstructural, Morphological, Optical Properties and Surface Electronic Structure of Copper Oxide Thin Films." *Materials Chemistry and Physics* **147**, 3 (2014) 987–95. <https://doi.org/10.1016/j.matchemphys.2014.06.047>.
- [34] Qu, Yongtao, Guillaume Zoppi, & Neil S. Beattie. "The Role of Nanoparticle Inks in Determining the Performance of Solution Processed Cu₂ZnSn(S,Se)₄ Thin Film Solar Cells." *Progress in Photovoltaics: Research and Applications* **24**, 6 (2016) 836–45. <https://doi.org/10.1002/pip.2756>.
- [35] Al-Ani, Salwan K. J., Raid A. Ismail, & Hana F.A. Al-Ta'ay. "Optoelectronic Properties n:CdS:In/p-Si Heterojunction Photodetector." *Journal of Materials Science: Materials in Electronics* **17**, 10 (2006) 819–24. <https://doi.org/10.1007/s10854-006-0028-x>.

